Deposition of nonsarcomeric alpha-actinin in cardiomyocytes from patients with dilated cardiomyopathy or chronic pressure overload

Stefan Hein MD[1], Tim Block MD[2], René Zimmermann PhD[2], Sawa Kostin[2], Thomas Scheffold MD PhD[3], Thomas Kubin PhD[2], Wolf-Peter Klövekorn MD PhD[1], Jutta Schaper MD PhD[2]

S Hein, T Block, R Zimmermann, et al. Deposition of nonsarcomeric alpha-actinin in cardiomyocytes from patients with dilated cardiomyopathy or chronic pressure overload. Exp Clin Cardiol 2009;14(3):e68-e75.

Nonsarcomeric alpha-actinin (ACTN-1)-positive clusters have been detected in human myocardium structurally jeopardized by dilated cardiomyopathy, hypertrophy due to aortic stenosis, or chronic hibernation, but have never been detected in normal tissue. To systematically investigate these clusters, immunohistochemistry, electron microscopy, Northern blot and Western blot were performed in human myocardium, isolated rat cardiomyocytes and rabbit smooth muscle cells. ACTN-1-positive clusters were localized in the perinuclear area of cardiomyocytes surrounded by rough endoplasmic reticulum. Quantification of structures containing ACTN-1 showed that it was present in up to 10% of all myocytes in 60% of aortic stenosis patients with severely reduced ejection fraction and in 70% of patients with dilated cardiomyopathy, exclusively in myocytes from hearts with structural degeneration and reduced function. Ultrastructurally, clusters of medium electron density corresponding to the confocal microscopic accumulations were observed in the same tissue samples. The messenger RNA of ACTN-1 was unchanged compared with controls, but a Western blot revealed that the protein was significantly elevated in failing hearts. Because membranes of the endoplasmic reticulum surround the clusters, it was concluded that in the presence of undisturbed transcription, a post-translational malfunction of ACTN-1 glycosylation might lead to storage of this protein. Autophagic and ischemic cell death were observed, but a possible toxic effect of this storage product was excluded because markers of cell death rarely colocalized with ACTN-1. The occurrence of ACTN-1-positive clusters, however, appears to be a useful marker for structural degeneration in failing myocardium.

Key Words: *ACTN-1; Cardiac failure; Human myocardium; Nonmuscle alpha-actinin*

Over the past decades, our group has extensively studied the morphological correlates of diastolic and systolic dysfunction in human heart failure caused by various cardiac diseases including dilated cardiomyopathy, myocarditis, hibernating myocardium and cardiac hypertrophy due to aortic stenosis (1-3). The development of fibrosis was identified as the primary cause of reduced diastolic function, and systolic dysfunction was associated with structural degeneration of the myocytes including alterations in the nuclei and the contractile apparatus, the cytoskeleton and the sarcolemmal components. In the course of these immunohistological studies, clusters containing smooth muscle alpha (α)-actinin were observed in failing myocardium. Simultaneously, using an electron microscope, we found that material of medium electron density were deposited in the nuclei and in the perinuclear area of myocytes in the same tissue samples from failing hearts.

The α-actinin gene family is part of the spectrin superfamily, and the approved gene symbol for α-actinin is *ACTN* (4). Alpha-actinin is a ubiquitously conserved protein that is able to cross-link actin filaments in skeletal and cardiac muscle as well as in nonmuscle cells in any orientation, with a preference for bipolar cross-linking (5). It is an antiparallel dimer consisting of two identical polypeptide chains with a molecular weight of 94 kDa to 103 kDa. Four different but closely related α-actinin genes and four different protein isoforms are known (ACTN-1, ACTN-2, ACTN-3 and ACTN-4). ACTN-1 is the nonmuscle-specific isoform that has, in addition to actin, more than 20 binding partners in stress fibres, focal adhesions and the cytoskeleton, as well as in adherens, tight junctions and others (6,7). Nonmuscle isoforms contain two functional helix-loop-helix (EF-hand) motifs that bind Ca^{2+} and are active in actin binding, while ACTN-2 and ACTN-3 bind actin in a Ca^{2+}-independent manner (8). Similar to ACTN-2 and ACTN-3, the incorporation of the actinin isoform ACTN-1 into the cytoskeleton is regulated by phosphoinositide phosphates (PIPs); the binding of ACTN to PIP_2 or PIP_3 decreases actin binding and increases gelation properties of ACTN-1 (9,10). However, in cardiac myocytes, ACTN-1 and ACTN-2 do not seem to be part of the cytoskeleton (own observations). Proteolysis of ACTN-1 is induced by calpain and this effect is dependent on phophoinositide binding to the substrate (11,12). Calpain-2 cleavage removes the actin-binding domain of α-actinin, which is important for cell adhesion and migration (12).

ACTN-2 occurs in heart and skeletal muscle, whereas ACTN-3 is found only in skeletal muscle. ACTN-4 represents a newly discovered nonmuscle isoform that still requires further investigation. In cardiac muscle, ACTN-1 and the sarcomeric ACTN-2 are of interest. In the myocardium, ACTN-1 normally occurs in the endothelium and media of blood vessels but not in other cells; it is detected predominantly in dense bodies and plaques, which are characteristic of nonmuscle cells. ACTN-2 is localized at the sarcomeric Z-disc, where it binds to titin and actin, thereby contributing to the stability of the

[1]*Kerckhoff Clinic;* [2]*Max-Planck-Institute for Heart and Lung Research, Bad Nauheim;* [3]*Institute for Heart and Circulation Research, University of Witten/Herdecke, Witten, Germany*

Correspondence: Dr Stefan Hein, Department of Cardiac Surgery, Kerckhoff-Clinic, Benekestrasse 2-8, D-61231 Bad Nauheim, Germany. Telephone +49-6032-996-2824, fax +49-6032-996-2456, e-mail stefan.hein@mpi-bn.mpg.de

Received for publication June 28, 2009. Accepted July 27, 2009

sarcomeric structure (13-15). ACTN-2 is also present in the intercalated disc. Despite the high degree of homology, specific antibodies are available to differentiate between ACTN-1 and ACTN-2: in Western blot and immunohistochemistry, monoclonal BM-75 stains ACTN-1 exclusively, and monoclonal EA-53 stains ACTN-2 and ACTN-3. EA-53 staining produces a clear cross-striation pattern, and is therefore an excellent marker of sarcomeric integrity and useful as an indicator of sarcomeric degeneration (3).

In our work on structural alterations in failing myocardium, ACTN-1 accumulations were typically seen in samples from patients with longstanding cardiac disease, but their occurrence was independent of the pathogenetic processes finally causing heart failure.

To study this phenomenon systematically, myocardium from one cohort of patients with heart failure due to dilated cardiomyopathy (DCM) and one with aortic valve stenosis displaying various degrees of severity of reduced cardiac function were analyzed by confocal and electron microscopy as well as by molecular biological methods for the quantitative aspect of the occurrence of the ACTN-1 clusters, their possible elimination by the ubiquitin-proteasome system and their relationship to the occurrence of cell death (16-18). The possible role of this protein in failing myocardium is discussed. Although the effect of storage of this nonmyocyte protein is currently unknown, it is worthwhile to report this phenomenon in the hope of initiating further studies on the role of this protein in structural degeneration.

METHODS

Patients

A group of 20 patients with DCM who had intractable heart failure and therefore underwent transplantation was studied. Furthermore, a group of 60 patients with aortic valve stenosis (AS) who had undergone operative valve replacement was investigated. The patients were subdivided into three groups (AS-1, AS-2 and AS-3) depending on their preoperative ejection fraction. Routine clinical evaluations, including echocardiography and catheterization, were performed. Clinical data are indicated in Table 1. The study was approved by the institutional ethics committee and all patients gave informed consent.

Data on these groups of patients, describing the typical structural changes and different types of cell death in the failing myocardium, were recently published (3,18).

TABLE 1
Clinical characteristics of the patient population

	Group				
Characteristic	Control	DCM	AS-1	AS-2	AS-3
EF, %	>50	<20	>50	50–30	<30
n	4	20	20	20	20
Men/women, n	4/0	16/3	8/12	8/12	9/11
EF, %	63±4	16±4	59±8	41±5	24±5
Age, years	48±10	51±8	70±6	67±12	71±7
PAP, mmHg	16±9	30±9	19±4	18±5	30±8
LVEDP, mmHg	7±4	29±9	15±5	18±6	24±5
LVEDD, mm	46±4	70±6	45±7	48±6	55±6
Delta P, mmHg	0	0	62±17	58±14	47±17
NYHA class	0	3.6±0.6	2.3±0.8	2.5±0.7	3±0.5

Data presented as mean ± SD unless otherwise indicated. All patients with dilated cardiomyopathy (DCM) were treated with digitalis, angiotensin-converting enzyme inhibitors, beta-blockers and diuretics at individual dosages. Additionally, depending on the individual situation, patients were treated with antiarrhythmic drugs. AS Aortic stenosis; EF Ejection fraction; LVEDD Left ventricular end-diastolic diameter; LVEDP Left ventricular end-diastolic pressure; NYHA New York Heart Association; P Pressure; PAP Pulmonary arterial pressure

Controls

Control group 1: Samples from six human hearts not suitable for transplantation.

Control group 2: Smooth muscle cells isolated from rabbit aorta were used as positive controls. After sacrifice of the animal, part of the aorta was removed and endothelial cells were destroyed by incubation in 70% alcohol. Afterwards, the cells were digested in Hank's balanced salt solution containing 0.05% collagenase plus 0.025% elastase (CellSystems, Germany). The cells were incubated in 5% CO_2 and 95% O_2 at 37°C for approximately two weeks until confluency (the same procedure as that used for porcine smooth muscle cells described by Kubin et al [19]).

Control group 3: Adult rat cardiomyocytes (ARCs) were isolated following routine procedures and kept in culture for three days (20). A Ca^{2+}-free perfusion was followed by perfusion with collagenase solution containing 0.03% collagenase (CLS-2, Worthington Biochemical Corporation, USA), 0.004% pronase (Boehringer Mannheim, Germany), 0.005% trypsin (Sigma-Aldrich Co, Germany) and 0.04 mM $CaCl_2$. The ventricles were minced and the cut pieces were added to the collagenase solution containing 1.2% bovine serum albumin (Sigma-Aldrich Co) for further digestion. After centrifugation and additional washing steps with three increments of Ca^{2+}, the cells were seeded in culture medium (Medium 199, Sigma-Aldrich Co) and analyzed after three days in culture.

Control group 4: Recombinant isoform-unspecific α-actinin with a weight of 98 kDa (A9776, Sigma-Aldrich Co).

Tissue sampling and fixation

Tissue samples were obtained by dissection of explanted hearts from patients with DCM. In patients with aortic valve defects, samples were taken from the left subvalvular septum during valve replacement. All tissues were immediately frozen in liquid nitrogen and stored at –80°C until further use. In addition, small samples from the same areas were fixed in 3% buffered glutaraldehyde for electron microscopy. Cultured cells were fixed in 3% paraformaldehyde.

Electron microscopy

The tissue was embedded in Epon following routine procedures. Ultrathin sections were double-stained with uranyl acetate and lead citrate, and viewed using a Philips (USA) CM-10 or CM-201 electron microscope.

Immunolabelling and confocal microscopy

Cryosections (5 µm thick) were air dried and fixed with paraformaldehyde or acetone. The primary antibodies used were monoclonal mouse antibody EA-53 for sarcomeric α-actinin (ACTN-2) (Sigma-Adrich Co) and BM-75.2 for smooth muscle α-actinin (ACTN-1) (Sigma-Aldrich Co). The latter was an immunoglobulin (Ig) M antibody, allowing for double-staining procedures with IgG monoclonal antibodies such as

TABLE 2
Antibodies and fluorochromes

Clone	Antigen	Host	Dilution	Immunglobulin (Ig)
EA-53	Rabbit skeletal α-actinin	Mouse	1:200	IgG1
BM-75.2	BMGE cultured cells α-actinin	Mouse	1:100	IgM
Poly	Chicken stomach α-actinin	Rabbit	1:100	Whole serum
Poly	Ubiquitin	Rabbit	1:50	Affinity purified serum
Poly	Human placenta collagen VI	Rabbit	1:150	Affinity purified serum
C9	Human C9	Mouse	1:100	IgG

Double and triple staining was performed using fluorochrome-labelled second antibodies or biotinylated second antibodies, and fluorochrome-labelled streptavidin. Fluorochromes: FITC, TRITC, TOTO-3, CY-3 and CY-5. Nuclear staining: Actinomycin and TOTO. BMGE Bovine mammary gland epithelium; C9 Complement 9

EA-53. Furthermore, whole rabbit antiserum against α-actinin from chicken stomach was used (Sigma-Aldrich Co). To identify ubiquitin, a polyclonal rabbit antibody (Dako, USA) and a monoclonal mouse antibody for complement 9 (C9, Novacastra, United Kingdom) were used (Table 2). For apoptosis, in situ labelling of fragmented DNA was performed using a commercially available kit (Boehringer Mannheim). The specificity of all antibodies was verified by omission of the first antibody, and by staining rabbit aortic smooth muscle cells and ARCs.

The secondary detection system was biotinylated antimouse or antirabbit either directly conjugated with Cy-2 or Cy-3, or unconjugated followed by FITC-linked streptavidin (Amersham, Germany). Myocyte identification was performed with TRITC-labelled phalloidin (Sigma-Aldrich Co). Nuclei were stained with either propidium iodide, DAPI or TOTO-3 (Molecular Probes, Invitrogen Corporation, USA).

The number of cells positive for BM-75.2, ubiquitin, C9 or TUNEL (single or in combination) were counted using a light microscope (Leica DM, Germany) following routine procedures (18).

Double labelling with the ubiquitin and BM-75.2 antibodies occasionally showed colocalization of ubiquitin in the α-actinin-positive granules. To generate histograms of these phenomena, small regions of interest were defined in confocal data sets. From these three-dimensional cubes representing 8000 voxels (20 mm × 20 mm × 20 mm) of the entire confocal data, the labelling in two different colours and the colocalization in the histogram with a specific distribution could be determined.

Picture acquisition was performed with a Leica confocal microscope (confocal laser scanning microscopy). Data were transferred to a Silicon Graphics workstation (Bitplane software, USA) for further processing and recording.

Western blot

For Western blot analysis, the EA-53 and the monoclonal and polyclonal BM-75.2 antibodies were used. Sodium dodecyl sulfate polyacrylamide gel electrophoresis (separating gels 12%) and immunoblotting were performed following routine protocols. For each lane, 30 µg of protein was loaded. GADPH with a size of 36 kDa was used as a reference protein.

Quantification was performed by densitometry, either using the gel-analyzing program Quantity One (Protein Imageware System Inc, USA) or scanning the immunoblots on a STORM 860 imager (Amersham Pharmacia Biotech, Germany) using ImageQuant software. All of the data were expressed as mean ± SEM. Statistical analysis by unpaired *t* test was considered significant at $P<0.05$.

Myocardial samples from three donors – rabbit aortic smooth muscle cells, ARC and recombinant α-actinin – served as controls.

Northern blot

Total RNA from a human left ventricle was isolated according to standard procedures (21). For Northern hybridization, 15 µg total RNA from ventricles of patients with DCM and from normal human hearts was separated on 1% agarose gel containing 0.66 M formaldehyde and transferred to a nylon membrane (Hybond N, Amersham Biosciences, Germany). The blots were hybridized with P-32 dCTP random-primed labelled complementary DNA (cDNA) probes (Rediprime II, Amersham Biosciences) or [32-P]ATP-labelled oligonucleotides. The blots were scanned using a Storm 860 PhosphorImager (Amersham Biosciences). For Northern blot analysis of the 18S ribosomal RNA, which was used for normalization, blots were rehybridized with a specific oligonucleotide as described previously (22). Quantification of the signals was performed using ImageQuant software (Amersham Biosciences). All of the experiments were repeated independently three times.

The following molecular probes were used for Northern blot analysis: ACTN-1 (own polymerase chain reaction [PCR] product), ACTN-2 (PCR product, J Ventre, National Institutes of Health, USA) and an 18S ribosomal RNA probe (own PCR product). Furthermore, to avoid the isoform similarity of the cDNA probes, oligonucleotides for ACTN-1 and ACTN-2, with significant differences in their messenger RNA (mRNA) sequence, were selected from a public library and cDNA probes were commercially produced (MWG Biotech Ebersberg, Germany).

mRNA levels were quantified using PhosphorImager and ImageQuant software (Molecular Dynamics, USA). For normalization, the data from each hybridization signal was divided by the matching 18S signal. All data were calculated as the percentage of control and presented as mean ± SEM or mean ± SD. Expression was assessed by an unpaired *t* test. Statistical significance was accepted at $P<0.05$.

RESULTS

Electron microscopy

Compared with normal myocardium, the tissue in most patients showed medium to severe myocyte degeneration, as previously described (Figure 1). This included the disappearance of sarcomeric material as well as mitochondrial and nuclear abnormalities (3,23).

Ultrastructurally, five of 17 patients with DCM showed accumulations of medium electron density of various sizes in the perinuclear area and within the nuclei (Figures 2A to 2C). The perinuclear structures were usually surrounded by intact or disrupted rough endoplasmic reticulum (ER), but sometimes, no membranous boundary could be seen. They were situated either in the cytoplasm or between the sarcomeres. Numerous nuclei showed enlargement, deformation and invaginations, and contained multiple elements of the ER. The nuclear membrane or rough ER surrounded the intranuclear clusters (Figure 2D). Frequently, the accumulations displayed dot-like depositions of dark substances, presumably phospholipid

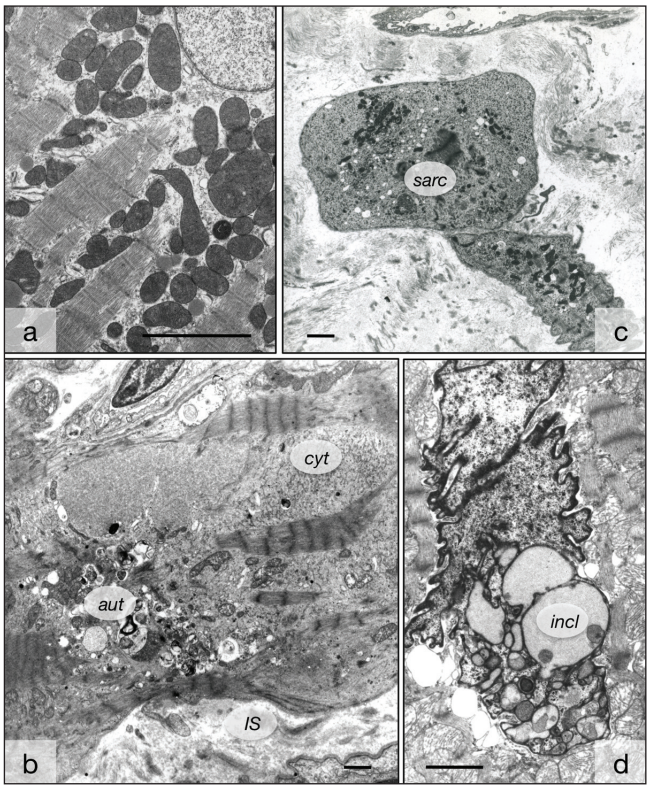

Figure 1) *Ultrastructural evidence of myocyte degeneration in human hearts*. **A** *Control myocardium with regular arrangement of sarcomeres*. **B** *Failing myocardium exhibits areas free of contractile material filled with nonspecific cytoplasm (cyt) and numerous autophagic vacuoles (aut). The interstitial space (IS) is widened*. **C** *Remnants of two cardiomyocytes with severe degeneration characterized by the presence of only a few contracted sarcomeres (sarc)*. **D** *Nuclear degeneration with invaginations, vacuoles and inclusions of material of light electron density (incl). Bars represent 5 µm*

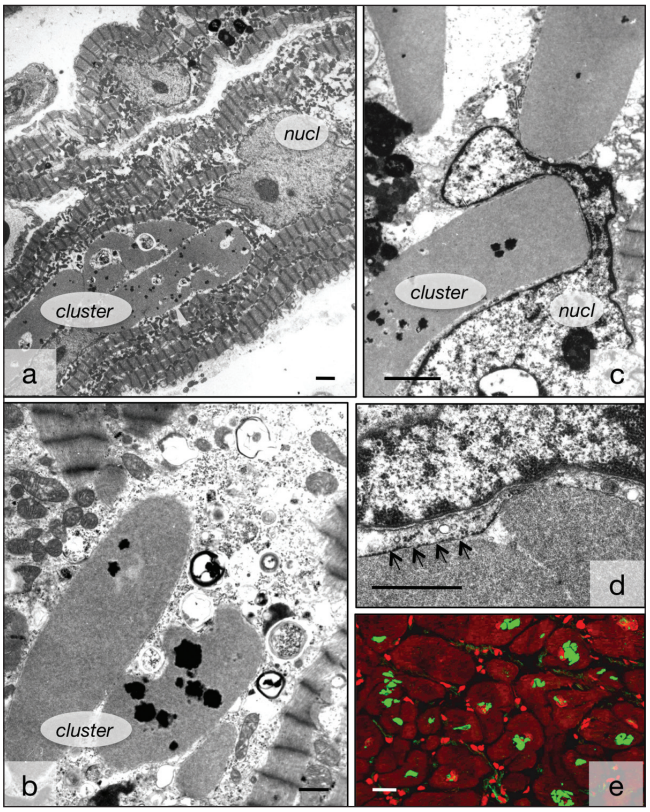

Figure 2) *Ultrastructural appearance of medium-density deposits of smooth muscle alpha-actinin*. **A** *Several clusters of smooth muscle alpha-actinin are situated in close proximity to the nucleus (nucl)*. **B** *Several clusters in the cytoplasm containing dark phospholipid dots*. **C** *Clusters compress the nucl*. **D** *The clusters are surrounded by endoplasmic reticulum (arrows). Bar represents 2 µm*. **E** *Appearance of the clusters by immunoconfocal microscopy. BM-75.2-positive structures are green and the myocytes are red with phalloidin. Red spots are interstitial cells. Bar represents 20 µm. Bars in* **A**, **B** *and* **C** *represent 5 µm*

material. This corresponded to the patients in which ACTN-1-positive clusters were observed by confocal microscopy (Figure 2E).

Immunohistochemistry

Characteristics of antibodies: The first step was to test the specificity of the different antibodies. The antibody EA-53 showed a clear sarcomeric cross-striation in isolated ARCs and in the control myocardium, and it revealed a disturbance in the cross-striation of the myocytes or the presence of EA-53-positive accumulations in diseased myocardium, which corroborated with the ultrastructural diagnosis of myocyte degeneration (Figure 3A). This confirmed the specificity of the antibody EA-53.

The polyclonal antibody against α-actinin labelled both spot-like or larger intracellular clusters in the myocytes and in the sarcomeres, indicating that the antiserum was not specific for either sarcomeric or smooth muscle α-actinin (Figure 3B).

The antibody BM-75.2 colocalized with actin-positive filaments of the cytoskeleton of smooth muscle cells in culture, proving its specificity for smooth muscle α-actinin (Figure 3C).

In experiments using colabelling with EA-53 and BM-75.2 (made possible by the fact that one antibody was IgM and the other IgG; therefore, the detection system could be specific), it was evident that EA-53 stained sarcomeric α-actinin and that BM-75.2 stained a large cluster of ACTN-1 in a myocyte, whereas the cytoskeleton remained unstained (Figure 3D).

A qualitative Western blot confirmed these immunohistochemical findings (Figure 3E).

Smooth muscle α-actinin in myocardium: The antibody BM-75.2 labelled blood vessels (Figures 4A and 4C) and identified the electron-dense clusters as ACTN-1, the smooth muscle-specific isoform of α-actinin (Figures 4B, 4D and 4E). ACTN-1-positive clusters were usually small but multiple structures were frequently found within one particular cell. The presence of multiple structures and small intranuclear positive spots corresponded with the electron microscopic findings.

The mRNA for ACTN-1 remained unchanged in the control versus diseased hearts in patients with DCM (Figure 5A). All three oligonucleotides used for the specific detection of ACTN-1 mRNA showed signals for both groups without statistically significant differences (data not shown).

The Western blot for ACTN-1 in patients with DCM showed a significant 14-fold upregulation of this protein in

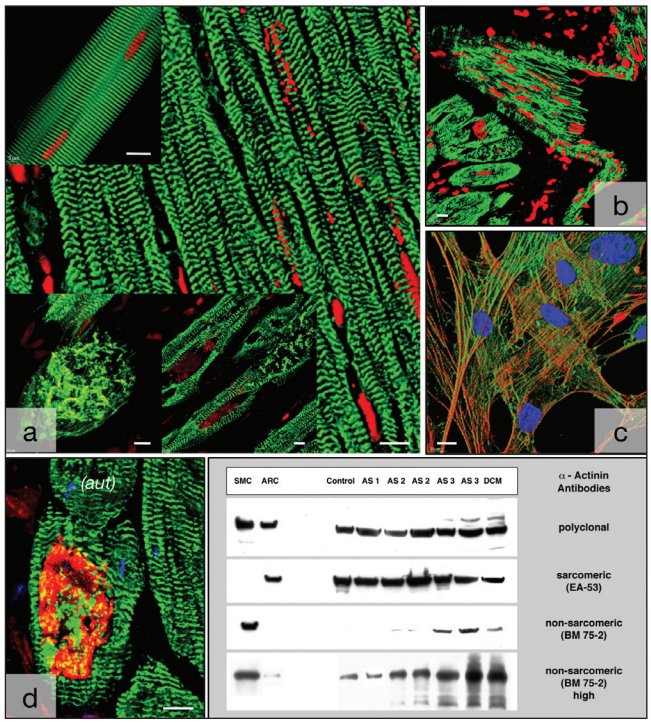

Figure 3) *Specificity of antibodies.* **A** *The antibody EA-53 for sarcomeric alpha (α)-actinin (green) reveals a distinct cross-striation in isolated myocytes (top left) and in normal myocardium (right). It shows disarrangement of sarcomeric α-actinin in failing myocardium (bottom). Nuclei are red.* **B** *The polyclonal antibody (green) stains blood vessels as well as myocytes. Nuclei are red.* **C** *The antibody BM-75.2 (green) colocalizes with the actin cytoskeleton (red) in cultured smooth muscle cells. Nuclei are blue. Shadow projection in the confocal microscope.* **D** *Colabelling of EA-53 (green) and BM-75.2 (red) shows a large smooth muscle α-actinin cluster surrounded by slightly disarranged sarcomeric α-actinin containing myofibrils. Nuclei are blue.* **E** *Western blot confirming the specificity of the antibodies used. Note the appearance of a slight band in adult rat myocytes (ARCs), controls and aortice stenosis (AS)-1 with longer exposure times (high). Aut Autophagic vacuoles; DCM Dilated cardiomyopathy; SMC Smooth muscle cells. Bars represent 10 μm*

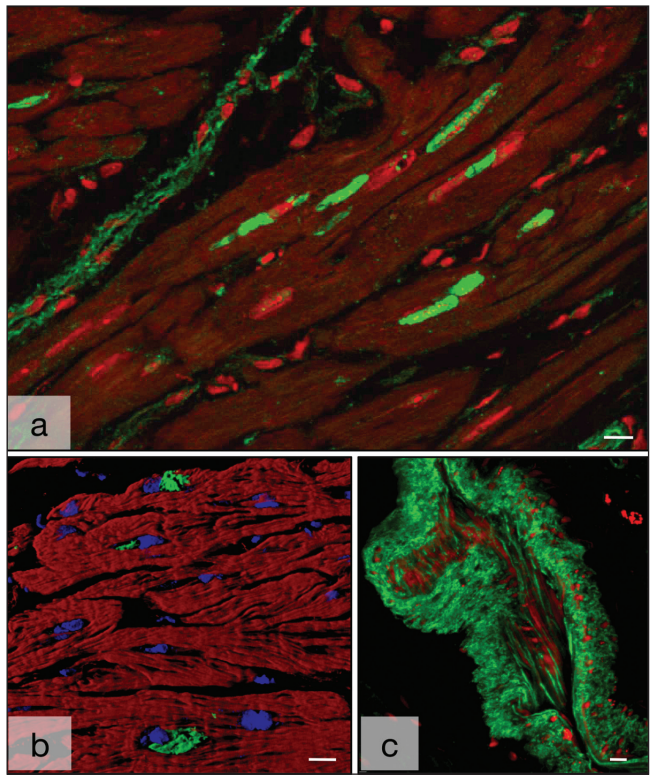

Figure 4) *Nonsarcomeric alpha (α)-actinin in human myocardium.* **A** *Several deposits of smooth muscle α-actinin (ACTN-1) (green) are in close proximity to the nucleus (red) in a longitudinal section of failing myocardium with dilated cardiomyopathy (red). Myocytes are dark. Note the labelling of blood vessels (top left).* **B** *ACTN-1-positive granules (green) are in close proximity to the nuclei (blue). Myocytes are red with phalloidin. Shadow projection in the confocal microscope.* **C** *Nonsarcomeric α-actinin in a tangentially sectioned arterial blood vessel. Faint staining of endothelial cells and strong labelling of the smooth muscle cells of the media (green). Nuclei are red. Bars represent 10 μm*

failing myocardium (Figure 5B). Sarcomeric α-actinin, detected with the EA-53 antibody, was present in both the control and DCM tissue without significant differences.

Quantification of the occurrence of BM-75.2-positive granules revealed the absence of any granules in the controls and AS-1 patients, a small number of clusters in AS-2 patients, and a significant increase of up to 3.7% in AS-3 and 4.9% in DCM patients (mean value for all patients; Figure 5C and Table 3). It is important to note that the numbers varied significantly from patient to patient, which resulted in a high SD.

Cell death: Labelling for ubiquitin usually filled the entire cell and the nucleus was frequently absent, indicating autophagic cell death (Table 3 and Figure 6A). In a total of 109 BM-75.2-positive myocytes in DCM, only five cells showed colocalization with ubiquitin (Figure 7). A similarly small number of cells simultaneously positive for ubiquitin and BM-75.2 was found in patients with AS. In general, patients positive for ubiquitin failed to show BM-75.2-positive granules, which further supported the conclusion that ACTN-1 is stored in myocytes but apparently is not toxic and is not involved in provoking cell death.

The number of cells undergoing ischemic cell death (oncosis) was 10 times higher than that of autophagic cell death, but it was still very low (Table 3 and Figure 6B). Apoptosis was found at an even lower rate and is therefore indicated as ‰ in Table 3.

It is of interest to note that the number of BM-75.2-positive cells was approximately 10 times greater than that for ubiquitin or C9. Furthermore, it was evident that both markers for cell death were slightly positive in the controls and AS-1 patients, and the increase was strongly correlated with the decrease in cardiac function. In contrast, BM-75.2-positive structures only occurred in failing myocardium. These observations further indicate that the occurrence of BM-75.2 is most likely not related to the incidence of cell death.

DISCUSSION

In the present report, the occurrence of smooth muscle α-actinin (ACTN-1) was described in cardiac myocytes from failing human hearts detected by electron and confocal

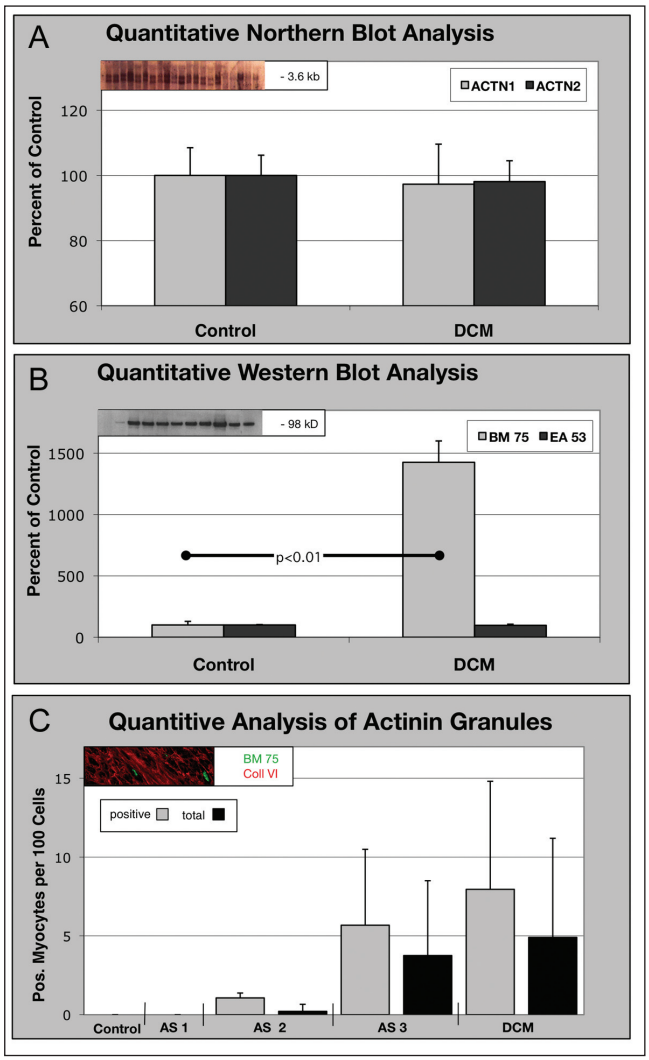

Figure 5) *Quantification of BM-75.2-positive granules in all patients (total) and positive patients (only patients with clusters) (see text).* **A** *Northern blot of smooth muscle alpha (α)-actinin (ACTN-1) and sarcomeric α-actinin (ACTN-2) messenger RNA in tissue with dilated cardiomyopathy (DCM). The amount of messenger RNA is unchanged in failing myocardium compared with controls.* **B** *Western blot using EA-53 and BM-75.2 antibodies in tissue from DCM. The content of ACTN-2 remains unchanged, whereas the BM-75.2-positive ACTN-1 increases significantly, corresponding with the structural results in* **C**. **C** *AS-1, AS-2 and AS-3 indicate stages of aortic stenosis severity. In the microscope, clusters were present in minimal amounts in AS-1 and AS-2, but they were numerous in AS-3 and DCM. There is, however, no statistically significant difference between the groups because of the high SD*

microscopy, and by Western and Northern blots. The data showed that transcription of ACTN-1 did not vary in normal versus diseased hearts, and that translation of BM-75.2-positive material is most likely not disturbed. However, the turnover of ACTN-1 seems to be significantly impaired, resulting in intracellularly stored clusters of this material. The present report also described the occurrence of myocyte cell death in failing hearts, and we hypothesized that storage of an abnormal non-sarcomeric protein would lead to death of the afflicted cell.

TABLE 3
Number of myocytes positive for different types of cell deaths* and for BM-75.2

	Group				
Protein	**Control**	**AS-1**	**AS-2**	**AS-3**	**DCM**
Ubiquitin,%	0.05±0.01	0.05±0.003	0.1±0.04†	0.6±0.005†	0.08±0.005
C9, %	0.0	0.3±0.05†	0.50±0.08†	0.40±0.03†	0.06±0.001†
Apoptosis, ‰	0.0	0.02±0.002	0.01±0.003	0.0	0.02±0.005
BM-75.2 total, %	0.0	0.0	0.2±0.4	3.7±4.7	4.9±6.2
Positive only, %			1.0 ±0.3	5.7±4.8	7.9±6.8
Number of patients, total/positive	6/0	20/0	20/4	20/12	20/14

*Data presented as mean ± SD unless otherwise indicated. *Data on cell death in the aortic stenosis (AS) and dilated cardiomyopathy (DCM) groups have been published recently (3,18); †P<0.05. C9 Complement 9*

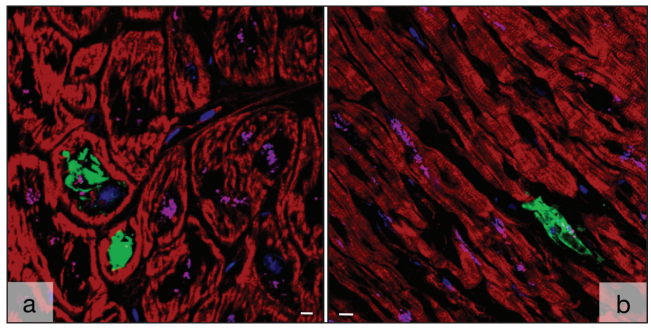

Figure 6) *Cell death in failing human myocardium.* **A** *Localization of ubiquitin in failing myocardium. Large deposits (green) are present within several myocytes. The nucleus in these cells is absent (blue in cells without ubiquitin). Myocytes are red with phalloidin.* **B** *Localization of complement (green) in failing myocardium*

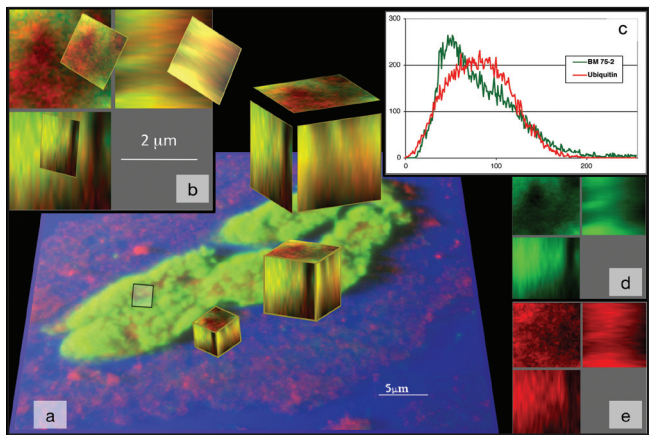

Figure 7) *Colocalization of ubiquitin (red) and BM-75.2 (green) in a myocyte from failing myocardium at a very high magnification.* **A** *The cluster was transformed in shadow projection and a small cube was defined.* **B** *The cube shows red, green and yellow compartments; yellow indicates colocalization.* **C** *Distribution of BM-75.2 (green) and ubiquitin (red) with slightly different maximum peaks and curve shapes.* **D** *and* **E** *Separation of the spectra resulting in the graph of* **C**

This, however, did not occur. Even though cell death (either by autophagy or necrosis) was observed, the incidence was 10 times lower than the incidence of BM-75.2 and was rarely

observed as colocalization. Based on these data, it can be speculated that post-translational disturbance of ACTN-1 glycosylation is the cause of the storage of this protein in failing myocytes but that this protein remains inert and not available for autophagic digestion.

Sarcomeric α-actinin commonly occurs at the Z-disc of sarcomeres in normal and diseased cardiac myocytes. It is an essential component of the contractile apparatus, where it significantly contributes to mechanotransduction, together with titin and many other proteins (24,25). In the present study, α-actinin was localized at the Z-disc and produced a distinct cross-striation of the myocytes. In diseased myocardium, irregular labelling and clusters of EA-53-positive structures, which is a sign of myocyte degeneration, were observed. In both Western and Northern blots, significant differences between normal and failing myocardium with regard to ACTN-2 were not evident, indicating that disorganization but not disturbances in the transcription and translation of this protein is a characteristic of failing myocardium.

The reliability of the observations reported in the present study depends on the specificity of the antibodies used. According to the manufacturer's product information, the immunogen for the antibody against the nonsarcomeric isoform of α-actinin was "the cytoskeletal fraction of bovine mammary gland epithelium (BMGE) cultured cells"; it is reported "to reveal extensive association of the proteins with actin containing stress fibers and in particular with their membrane bound termini" (literal citation from Sigma datasheet). The specificity of this antibody for smooth muscle α-actinin is clearly evident in the present study because myocytes of normal myocardium show no staining with BM-75.2 either in immunohistochemistry or Western blot. Blood vessels, however, are positive in myocardium determined by microscopy and are the cause of a slight band in the Western blot. This situation is different in failing hearts where the BM-75.2 is elevated 14-fold and where intracellular clusters of this protein are found by confocal microscopy. The control value was so low in the Western blot that a 14-fold increase may not be so excessive considering the rate of appearance in the microscope. In the present study, there was no evidence for cardiac myocytes of focal adhesions or cytoskeletal elements positive for BM-75.2. This is in contrast to Latif et al (26), who postulated that BM-75.2 would label the cytoskeleton of cardiomyocytes. However, this group based their statements on Western blot data and did not perform confocal microscopy. Therefore, the ultimate proof for the presence of BM-75.2-positive elements in the cytoskeleton or in focal adhesions is missing in their work.

It is of interest that in the present study, the mRNA levels of ACTN-1 remained unchanged in failing hearts, implicating that a post-translational disturbance might occur. In this context, it is important to note that ACTN-1 clusters were mostly surrounded by rough ER. Enzymes in the ER normally control post-translational modifications of secreted proteins because protein folding and maturation in the ER are essential for subsequent transport through the secretory pathway (27,28). We have found that ACTN-1 is stored in the ER and apparently not transported to the cytoplasm. The conclusion drawn from this finding is that the secretory pathway and therefore the ER-dependent quality control of protein synthesis is defective, resulting in accumulation of ACTN-1. Furthermore, the intranuclear localization of ACTN-1 surrounded by nuclear or ER membranes could be caused by nuclear invaginations similar to the inclusion of mitochondria or cytoplasm described previously in myocytes from failing hearts (23).

Misfolded or unassembled proteins are usually degraded by the ubiquitin-proteasome system. This is most likely also the case for ACTN-1. To test this hypothesis, double-labelling with nonmuscle α-actinin and ubiquitin was performed. Five per cent of all myocytes were positive for ACTN-1, but the number of ubiquitin-positive granules was 10 times lower. Careful analysis using the confocal microscope revealed that only five of 109 cells were labelled for both proteins. It was therefore concluded that in failing myocytes, ACTN-1 is not secreted into the cytoplasm but remains in storage in the ER. Glycosylation of proteins by specific enzymes is likely to be the decisive factor for its secretion from the ER. Even small changes in the N-linked glycans prevent the protein from being recognized by the ER-associated degradation system and results in indefinite storage of the protein (29). This is consistent with the fact that ACTN-1 was absent in the myocytes of normal myocardium, which suggests that ACTN-1 is either immediately degraded in the ER or that it is not synthetized in normal myocytes. The results from the present Northern and Western blots favour the first possibility; ie, after synthesis, ACTN-1 is immediately removed from the ER by the intact ER-associated degradation system. This confirms the hypothesis presented above that in the myocytes from failing myocardium, the glycosylation status of ACTN-1 is disturbed, leading to storage of the protein.

A recent study (30) reported aggregation of ubiquitinated proteins in mouse hearts and showed that this phenomenon promotes autophagy. This is consistent with our findings regarding proteins, such as myosin, sarcomeric α-actinin or connexin-43, but it apparently does not apply for ACTN-1 (unpublished data). This is another strong indication that BM-75.2-positive material remains stored in the ER and is therefore not available for autophagic digestion. However, the fact that a small percentage of myocytes were positive for ubiquitin suggests that a certain number of cells undergo autophagic degeneration and later, cell death (17,18,31,32).

Oncosis, another type of cell death, is identified by C9 uptake, which occurs because of the leakiness of cellular membranes typical of ischemia. The percentage of cells found to be positive for C9 was 0.06% (ie, slightly higher than for autophagic cell death. Apoptosis was negligible. These numbers have been taken from earlier publications concerning patients with AS and DCM (3,18). Since the length of duration of ubiquitin or C9 deposition or of DNA fragmentation in myocytes is still unknown, it is almost impossible to define the absolute number of dying cells by any type of cell death (for a discussion on this problem, refer to Suzuki et al [33] and Kostin et al [18]).

BM-75.2 deposition was 10 times higher than the rates of cell death in the present study, and colocalization with the cell death markers ubiquitin or C9 was very rarely observed. This indicates that ACTN-1 is apparently not toxic to the cell where it is stored. Finally, it is important to note that various forms of cell death occur in diseased failing myocardium and that these apparently are unrelated to the deposition of ACTN-1.

REFERENCES

1. Elsasser A, Schlepper M, Klovekorn WP, et al. Hibernating myocardium: An incomplete adaptation to ischemia. Circulation 1997;96:2920-31.
2. Heling A, Zimmermann R, Kostin S, et al. Increased expression of cytoskeletal, linkage, and extracellular proteins in failing human myocardium. Circ Res 2000;86:846-53.
3. Hein S, Arnon E, Kostin S, et al. Progression from compensated hypertrophy to failure in the pressure-overloaded human heart: Structural deterioration and compensatory mechanisms. Circulation 2003;107:984-91.
4. Dixson JD, Forstner MJ, Garcia DM. The alpha-actinin gene family: A revised classification. J Mol Evol 2003;56:1-10.
5. Taylor KA, Taylor DW, Schachat F. Isoforms of alpha-actinin from cardiac, smooth, and skeletal muscle form polar arrays of actin filaments. J Cell Biol 2000;149:635-46.
6. Otey CA, Carpen O. Alpha-actinin revisited: A fresh look at an old player. Cell Motil Cytoskeleton 2004;58:104-11.
7. Sjoblom B, Salmazo A, Djinovic-Carugo K. alpha-Actinin structure and regulation. Cell Mol Life Sci 2008;65:2688-701.
8. Tang J, Taylor DW, Taylor KA. The three-dimensional structure of alpha-actinin obtained by cryoelectron microscopy suggests a model for Ca(2+)-dependent actin binding. J Mol Biol 2001;310:845-58.
9. Fraley TS, Tran TC, Corgan AM, et al. Phosphoinositide binding inhibits alpha-actinin bundling activity. J Biol Chem 2003;278:24039-45.
10. Fukami K, Furuhashi K, Inagaki M, Endo T, Hatano S, Takenawa T. Requirement of phosphatidylinositol 4,5-bisphosphate for alpha-actinin function. Nature 1992;359:150-2.
11. Franco S, Perrin B, Huttenlocher A. Isoform specific function of calpain 2 in regulating membrane protrusion. Exp Cell Res 2004;299:179-87.
12. Sprague CR, Fraley TS, Jang HS, Lal S, Greenwood JA. Phosphoinositide binding to the substrate regulates susceptibility to proteolysis by calpain. J Biol Chem 2008;283:9217-23.
13. Burridge K, Kelly T, Connell L. Proteins involved in the attachment of actin to the plasma membrane. Philos Trans R Soc Lond B Biol Sci 1982;299:291-9.
14. Sorimachi H, Freiburg A, Kolmerer B, et al. Tissue-specific expression and alpha-actinin binding properties of the Z-disc titin: Implications for the nature of vertebrate Z-discs. J Mol Biol 1997;270:688-95.
15. Clark KA, McElhinny AS, Beckerle MC, Gregorio CC. Striated muscle cytoarchitecture: An intricate web of form and function. Annu Rev Cell Dev Biol 2002;18:637-706.
16. Ciechanover A, Orian A, Schwartz AL. The ubiquitin-mediated proteolytic pathway: Mode of action and clinical implications. J Cell Biochem Suppl 2000;34:40-51.
17. Knaapen MW, Davies MJ, De Bie M, Haven AJ, Martinet W, Kockx MM. Apoptotic versus autophagic cell death in heart failure. Cardiovasc Res 2001;51:304-12.
18. Kostin S, Pool L, Elsasser A, et al. Myocytes die by multiple mechanisms in failing human hearts. Circ Res 2003;92:715-24.
19. Kubin T, Vogel S, Wetzel J, et al. Porcine aortic endothelial cells show little effects on smooth muscle cells but are potent stimulators of cardiomyocyte growth. Mol Cell Biochem 2003;242:39-45.
20. Person V, Kostin S, Suzuki K, Labeit S, Schaper J. Antisense oligonucleotide experiments elucidate the essential role of titin in sarcomerogenesis in adult rat cardiomyocytes in long-term culture. J Cell Sci 2000;113:3851-9.
21. Chomczynski P, Sacchi N. Single-step method of RNA isolation by acid guanidinium thiocyanate-phenol-chloroform extraction. Anal Biochem 1987;162:156-9.
22. Deindl E. 18S ribosomal RNA detection on Northern blot employing a specific oligonucleotide. Biotechniques 2001;31:1250,1252.
23. Schaper J, Froede R, Hein S, et al. Impairment of the myocardial ultrastructure and changes of the cytoskeleton in dilated cardiomyopathy. Circulation 1991;83:504-14.
24. Linke WA. Sense and stretchability: The role of titin and titin-associated proteins in myocardial stress-sensing and mechanical dysfunction. Cardiovasc Res 2008;77:637-48.
25. Samarel AM. Costameres, focal adhesions, and cardiomyocyte mechanotransduction. Am J Physiol Heart Circ Physiol 2005;289:H2291-301.
26. Latif N, Yacoub MH, George R, Barton PJ, Birks EJ. Changes in sarcomeric and non-sarcomeric cytoskeletal proteins and focal adhesion molecules during clinical myocardial recovery after left ventricular assist device support. J Heart Lung Transplant 2007;26:230-5.
27. Bukau B, Weissman J, Horwich A. Molecular chaperones and protein quality control. Cell 2006;125:443-51.
28. Wang X, Robbins J. Heart failure and protein quality control. Circ Res 2006;99:1315-28.
29. Helenius A, Aebi M. Roles of N-linked glycans in the endoplasmic reticulum. Annu Rev Biochem 2004;73:1019-49.
30. Tannous P, Zhu H, Nemchenko A, et al. Intracellular protein aggregation is a proximal trigger of cardiomyocyte autophagy. Circulation 2008;117:3070-8.
31. Nakai A, Yamaguchi O, Takeda T, et al. The role of autophagy in cardiomyocytes in the basal state and in response to hemodynamic stress. Nat Med 2007;13:619-24.
32. Shimomura H, Terasaki F, Hayashi T, Kitaura Y, Isomura T, Suma H. Autophagic degeneration as a possible mechanism of myocardial cell death in dilated cardiomyopathy. Jpn Circ J 2001;65:965-8.
33. Suzuki K, Kostin S, Person V, Elsasser A, Schaper J. Time course of the apoptotic cascade and effects of caspase inhibitors in adult rat ventricular cardiomyocytes. J Mol Cell Cardiol 2001;33:983-94.